Aalborg Universitet

Accelerated physical aging of four PET copolyesters

Enthalpy relaxation and yield behaviour

Weyhe, Anne Therese; Andersen, Emil; Mikkelsen, René; Yu, Donghong

[Link to publication from Aalborg University](#)

Accelerated physical aging of four PET copolyesters: Enthalpy relaxation and yield behaviour

Anne Therese Weyhe [a,b], Emil Andersen [b], René Mikkelsen [b], Donghong Yu [a,*]

[a] *Department of Chemistry and Bioscience, Aalborg University, Fredrik Bajers Vej 7H, DK-9220, Aalborg East, Denmark*
[b] *LEGO System A/S, Åstvej 1, DK-7190, Billund, Denmark*

ARTICLE INFO

ABSTRACT

Assessing suitability of amorphous polymers in durable products requires understanding of long-term effects of physical aging on the material properties. This work shows four polyesters with varying diol composition (poly (ethylene-co-1,4-cyclohexylenedimethylene terephthalate) (PETG1 and PETG2 with ~30 and ~60% 1,4-cyclo-hexylenedimethylene (CHDM), respectively), poly(ethylene-co-2,2,4,4-tetramethyl-1,3-cyclobutanediol tere-phthalate) (PETT) with ~30% 2,2,4,4-tetramethyl-1,3-cyclobutanediol (TMCD) and poly(1,4-cyclohexylenedimethylene-co-2,2,4,4-tetramethyl-1,3-cyclobutanediol terephthalate) (PCTT) with ~80% CHDM and ~20% TMCD) exposed to thermal treatment at 20, 30 and 40 °C below their respective glass transition temperatures for up to 504 h to accelerate physical aging. The enthalpy relaxation was investigated by differential scanning calorimetry and compared to mechanical changes manifested as tensile yield strength increase. The physical aging rates were found to depend on both chemical structure and composition of CHDM and TMCD segments, where the introduction of TMCD inhibited physical aging. Arrhenius and Vogel-Fulcher-Tamman models were used to fit horizontal shift factors and evaluate the time and temperature dependencies for each polyester. From this study, the two models showed no significant differences in ability to describe the effects of physical aging. The Arrhenius activation energies, E_a, were all in the range 118–244 kJ mol^{-1}, were both PETG1 and PETG2 showed no significant difference between E_a for enthalpy relaxation and yield strength increase, whereas PETT and PCTT showed ~19 and ~107% difference between the two, respectively, suggesting that the relationship between the two phenomena is not independent of chemical structure. The difference between the activation energies suggests that the time scales for physical aging are different when observed as enthalpy relaxation and yield strength.

1. Introduction

Amorphous and semi-crystalline polymers are an essential part of daily life and their significance in engineering applications increases as intensive research in this scientific area continuously improve material performance and properties [1–5]. Being a representative class of commercial polymers showing great potential regarding both sustainability [6,7] and mechanical properties [8], polyesters such as poly (ethylene terephthalate) (PET) has gained much attention. PET is used in beverage bottles, food packaging, and fibres, due to e.g. excellent food-safety and recycling properties [9,10] and, furthermore, the chemical modification of PET with different diols, can lead to improved mechanical [11] and barrier properties [12]. Incorporating 1,4-cyclo-hexylenedimethanol (CHDM) into PET backbone as illustrated in

Fig. 1a, first reported by Kibler et al. in 1959 [13], have led to ternary copolyesters with low crystallization rates and improved optical transparency, mechanical toughness and chemical resistance [14], which can be readily introduced into polyesters via high-temperature, melting state, and/or transition metal catalysed process with superior impact property owning to its conformation transition [14,15]. The glycol ratio of 30% CHDM and 70% EG has originally been chosen for commercialization as it exhibits the lowest crystallization rate compared to other CHDM/EG compositions [14]. This means that increasing the CHDM content further decreases the amorphous window and increases the ability to form ordered structures. Another promising diol, 2,2,4,4-tetra-methyl-1,3-cyclobutanediol (TMCD), has also been used to modify PET Fig. 1b increasing the glass transition temperature (T_g) due to the rigid structure of the cyclobutyl ring [16]. Incorporation with TMCD and

---

* Corresponding author.
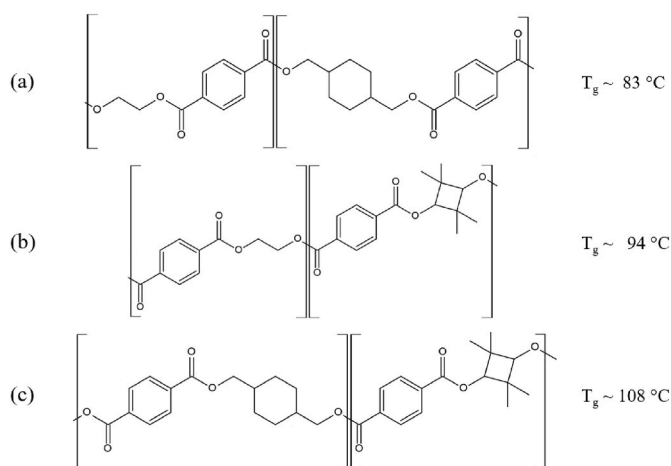*E-mail address:* yu@bio.aau.dk (D. Yu).

Fig. 1. Chemical structure of (a) poly(ethylene-co-1,4-cyclohexylenedimethylene terephthalate), (b) poly(ethylene-co-2,2,4,4-tetramethyl-1,3-cyclobutanediol terephthalate) (PETT) and (c) poly(1,4-cyclohexylenedimethylene-co-2,2,4,4-tetramethyl-1,3-cyclobutanediol terephthalate) (PCTT) along with their corresponding T_g.

CHDM monomer into a copolyester backbone also led to films with improved toughness and tear resistance compared to traditional polyester films [17]. On the other hand both CHDM and TMCD have been found as renewably sourced materials based on its naturally occurring camphor [18]. However, polyesters are often challenged in high temperature applications [19,20] and in durable products with long lifetime expectancies [21].

Physical aging is a central mechanism, which must be understood in the lifetime prediction of polyesters. Polymers in their glassy state, i.e. below T_g, are not in thermodynamic equilibrium, and their structures continuously approach a meta-stable or an equilibrium state [22]. This time and temperature dependent relaxation process is known as physical aging, causing both micro- and macroscopic changes on materials physical properties. On a molecular level, motions of individual atoms, molecules or segments cause secondary bond breakage and reformation during the structural relaxation [23]. Hence, various types of bonds and interactions are involved in the physical aging process that occurs after glass formation, which, due to the complexity, remain poorly understood. Macroscopically, physical aging of polymers causes an observable change in material properties e.g. enthalpy, free volume, viscosity, fracture toughness, E-modulus [24] and yield strength [20]. The description of the macroscopic relaxation behaviour has often been achieved through phenomenological models such as the Tool-Narayanaswamy-Moynihan (TNM) model, which takes the lead in describing complex relaxation features [25–27]. The TNM model describes the relaxation time as function of fictive temperature (T_f) rather than T_g, where T_f is defined as the temperature at which the glass is in the same state as the relaxed structure [25]. However, both T_g and T_f are readily used in literature to describe the temperature dependence of physical aging rate in glassy materials.

The possibility to predict the rate of physical aging and the effect on material properties is invaluable for the plastic industry. These changes can further influence the functionality of amorphous polymers and govern their applicability [14,16]. Therefore, the use of such amorphous polymers in durable products requires development of experimental methods and numerical models to characterize the long-term effects of physical aging on the mechanical properties to e.g. predict functionality, stability and ultimately lifetime. Several experimental investigations have already been carried out to understand the changes of mechanical properties during physical aging [23,24,28–30]. Differential scanning calorimetry (DSC) is a widely used technique to describe the influence of cooling rate and sub-T_g annealing time on enthalpy relaxation [23,28].

After annealing, the magnitude and peak position of endotherm overshoot around T_g increases, resulting in a quantitative measure of enthalpy lost upon annealing [29]. Another commonly used method to characterize physical aging is to measure the stress-strain response of specimens after different thermal treatments [24,30]. Hutchinson et al. showed that the yield strength of amorphous polycarbonate annealed for 1000 h at 125 °C ($\approx T_g$-20 °C) increased by approximately 20% compared to samples without annealing [30]. Yield strength increase and enthalpy loss are both ascribed to secondary bonds and attractions between polymeric segments, which must be broken in the glass transition upon heating or to reach the yield point of a stress-strain experiment. Therefore, it is realistically assumed, that the two phenomena are coupled and follow similar time and temperature dependency. However, several studies present contradictory results, where the enthalpic response and the change in mechanical properties do not follow each other. It has also been demonstrated that enthalpy and specific volume change do not follow the same kinetics at shorter aging times ($t < t_{eq}$) in polycarbonate, polystyrene and polyvinyl acetate, where t_{eq} is the annealing time necessary to remove the prior thermal history of the sample [19,30]. At $t < t_{eq}$ the specific volume was found to decrease while the enthalpy stayed constant, whereas the two follow the same kinetics at longer aging times ($t > t_{eq}$) [31].

To evaluate the temperature acceleration of aging and to extrapolate results to make long-term predictions, the Arrhenius approach has been traditionally used [32]. The method is based on the assumption, that aging is a thermally activated process with its rate proportional to exp ($-E_a/RT$), where E_a is the activation energy, R is the gas constant and T is the exposed temperature. The Arrhenius equation is expressed as:

$$k = A \exp\left[\frac{E_a}{RT}\right] \tag{1}$$

where k is the rate constant. If the aging process follows Arrhenius behaviour, shift factors will be related to E_a by the expression:

$$a_T = \exp\left[\frac{E_a}{R}\left(\frac{1}{T_{ref}} - \frac{1}{T}\right)\right] \tag{2}$$

where a_T is the shift factor corresponding to the shift from a test temperature, T, to a reference temperature, T_{ref}. The Arrhenius activation energies may be limited by the assumption, that they are temperature-independent, and hence, the activation energies might not be identical for all ranges of annealing temperatures with different proximity to T_g. Therefore, care needs to be taken, when extrapolating outside the tested time and temperatures [33]. Another widely used model to describe relaxation processes is the Vogel-Fulcher-Tamman (VFT) law [29,34], described by the function:

$$\tau = B \exp\left[\frac{D}{T - T_0}\right] \tag{3}$$

where τ is the relaxation time, B is the pre-exponential factor, D is a material dependent constant, the so-called Vogel activation energy, and T_0 is defined as the temperature with zero free volume or infinite relaxation time. Earlier studies by DiMarzio and Yang [35] and O'Connell and McKenna [36] show that changes in viscosity and viscoelastic properties follow VFT temperature dependence above T_g, but transitions to an Arrhenius type dependence as T_g is approached. Furthermore, several studies reported in more recent years show that physical aging experiments (below T_g) deviate from VFT behaviour to a milder temperature dependence in both mechanical and dielectric measurements [37] and for volume and enthalpy loss [38]. However, some studies have also showed that VFT law is retained even at temperatures below T_g. Boucher et al. and Richert both reported VFT behaviour in polyvinyl acetate in relaxation time [39] and time domain experiments [40], respectively. These studies were however carried out in closer proximity to T_g.

In this work we aim to increase the understanding of aging behaviour in new types of polyester. We apply DSC studies to quantify enthalpy relaxation in four different glycol modified PET grades after aging below their respective T_g values. Changes in tensile properties after aging are compared to those in enthalpy relaxation to investigate if the two properties exhibit similar time and temperature dependency, hence if the changes are caused by the same mechanism and can be extrapolated similarly for long-term predictions. Arrhenius and VFT law are used to evaluate the shift factors of the two separate properties. Finally, this work seeks to investigate how glycol modification of PET alters physical aging and whether chemical structure influences the correlation between enthalpy loss and yield strength increase.

2. Materials and methods

2.1. Materials

Granulate of poly(ethylene-co-2,2,4,4-tetramethyl-1,3-cyclobutanediol terephthalate) (PETT) (GMX201, Eastman, USA), poly (ethylene-co-1,4-cyclohexylenedimethylene terephthalate) (PETG1, PETG2) (GN007, DN011, Eastman, USA) and poly(1,4-cyclohexylenedimethylene-co-2,2,4,4-tetramethyl-1,3-cyclobutanediol terephthalate) (PCTT) (TX1001, Eastman, USA) (all structures shown in Fig. 1). The polyesters were injection moulded (Arburg 470E 600-290 Arburg, GER) to tensile test specimens (1BA, ISO 527–2:2012) under various conditions according to Table 1.

2.2. Nuclear magnetic resonance spectroscopy

10 mg of PETT, PETG1, PETG2 and PCTT were dissolved for 2 h in 0.8 mL a co-solvent of 25 vol% deuterated trifluoroacetic acid (99.5% TFAA-d, Sigma Aldrich, GER) and 75 vol% CDCl3 (99.8% Chloroform-d, Sigma Aldrich, GER). NMR spectrometer (Ascend 400 MHz, Bruker, USA) recorded 16 scans for ^1H spectra and 1024 scans for ^{13}C NMR spectra. Data analysis was performed in TopSpin (V. 4.1.3, Bruker, GER).

2.3. Attenuated total reflectance infrared spectroscopy

Spectra were collected from the grip section of tensile bars on FT-IR spectrophotometer (Thermo Scientific, iS50, USA) equipped with ZnSe ATR (iD5, Thermo Scientific, USA). Spectra averaged 8 scans in the wavenumber interval of 500–4000 cm^{-1}, with baseline corrected in OMNIC (v. 8.2.388., TA Scientific, USA).

2.4. Gel permeation chromatography

To determine average molecular weights and their distribution, gel permeation chromatography (GPC) was used. Calibration was performed with poly(methylmethacrylate) standards. A solution of 0.5 M potassiumtrifluoroacetate in hexafluoroisopropanol was used as both the eluent and solvent of samples (3 mg/mL at room temperature). All solutions were filtered through a 1 μm filter and 50 μL of those were injected by an autosampler (PSS SECcurity 1260 autosampler) at a flow rate of 1.00 mL/min into columns (PSS PFG, 7 μm, Guard, ID 8.00 mm × 50.00 mm) and 2x(PSS PFG linear M, 7 μm, ID 8.00 mm × 300.00 mm) at 30 °C.

2.5. Thermal treatment

Tensile bars and DSC samples were annealed in ovens at T_g-20, -30 and −40 °C for 0.5, 1, 2, 4, 8, 16 and 24 h, while samples at T_g-30 and -40 °C were treated for 168, 336 and 504 h, additionally. After thermal treatment, all samples were stored at room temperature for a least 24 h before testing.

2.6. Differential scanning calorimetry

Samples of 5–10 mg were cut from tensile bars, placed in pans (Tzero hermetic pan 901683.901, TA Instruments, USA) and covered with lids (Tzero hermetic lid 901683.901, TA Instruments, USA). Samples were measured in a DSC (Q2000, TA Instruments, USA) with nitrogen flow (50 mL/min). All samples were heated twice from 20 to 300 °C at 10 °C/min with their cooling to 20 °C at 10 °C/min in between. Samples were tested in triplicates.

The enthalpy loss ($\Delta H(T_g)$), caused by aging, was determined by the area difference of the endotherm peaks between annealed sample and the references at T_g [19].

2.7. Tensile testing

Test specimens were mounted with the inlet in the lower pneumatic grip in a universal testing machine (Z005, ZwickRoall, GER) with a 25 mm gauge length extensometer (180102/2008, ZwickRoell, GER) controlled by testXpert II (Zwick, GER). Test and data extraction were performed according to ISO 527–1 (tests were done in triplicates). Yield strength (σ_Y) was evaluated at 100 mm/min at 23 ± 2 °C.

2.8. Arrhenius and VFT fit

Arrhenius and VFT plots were prepared from shift factors (a_T) as function of reciprocal temperature of exposure. Horizontal shift factors for both yield strength and enthalpy relaxation were determined with T_g-40 °C as reference temperature (all data was shifted to match the best fit curve for the T_g-40 °C data set). Both sets of shift factors were subsequently fit with Arrhenius and VFT equations.

3. Results and discussion

3.1. Structural analysis

The chemical structures of the four different PET copolymers were characterized by means of ^1H NMR, ^{13}C NMR and ATR-FTIR, Figs. S1–17 and Tables S1–9. Glycol ratios of CHDM, TMCD and EG, determined by integrals of their corresponding peaks from ^1H NMR spectra, are

Table 2
Chemical composition of PETT, PETG1, PETG2 and PCTT along with number average molecular weight (Mn) determined by GPC.

	CHDM	TMCD	EG	M_n [kDa]
PETT	–	0.29	0.71	14.0
PETG1	0.31	–	0.69	14.8
PETG2	0.63	–	0.37	14.8
PCTT	0.78	0.22	–	13.4

Table 1
Moulding parameters for tensile bars of PETT, PETG1, PETG2, and PCTT.

	Moisture content [%]	Drying temp. [°C]	Drying time [h]	Melt temp. [°C]	Injection pressure [bar]	Mould temp. [°C]	Cooling time [s]
PETT	0.03	80	8	295	1150	80	20
PETG1	0.02	80	8	272	800	60	26
PETG2	0.02	80	8	275	800	60	25
PCTT	0.03	85	6	285	936	80	18

presented in Table 2 along with number average molecular weight (M_n) determined by GPC.

Both PETG1 and PETG2 contain CHDM and EG, where PETG2 contain roughly double the amount of CHDM compared to PETG1 (63 and 31%, respectively). PETT contain 29% TMCD, and thus contain approximately the same amount of EG as PETG1 (71 and 69%, respectively). PCTT contains no EG but only CHDM and TMCD. The M_n values are similar varying from 13.4 to 14.8 kDa, which does not affect thermodynamic properties more than 0–1%, according to the Flory Fox equation [41,42] Eq. S11-13.

Table 3 gathers values of T_g, T_f and ΔC_p determined from the first heating scans from DSC. PCTT exhibits the highest T_g, which can be expected from the increased steric hindrance in especially TMCD but also CHDM compared to EG. Furthermore, the high structural stiffness of TMCD is expressed in the T_g of PETT, which is ~13 °C higher compared to the T_g of PETG1 both containing ~30% glycol modification. Since the CHDM and TMCD segments disrupt the ordered structure of PET, when partially replacing EG, crystallinity was not expected in any of the samples. The amorphous nature was confirmed by DSC and x-ray diffraction spectroscopy, Figs. S9–13, showing no melting/crystallization or crystalline peaks, respectively, in any of the copolyesters.

The difference between T_g and T_f is 2 °C for PETT and the PETGs, whereas the difference is only 1 °C for PCTT. This means that the so-called structural temperature is close to T_g in all the polyesters, and that T_g and T_f are equally good references for physical aging in this study. The obtained values of ΔC_p are similar for all the polyesters and correspond well with previous studies [43]. From these values it can be presumed that the excess energy related to free volume is similar [44,45] suggesting that the thermodynamic force for enthalpy relaxation sub-T_g is likewise similar in the four polyesters [44].

3.2. Enthalpy relaxation

Sets of DSC traces for samples of PETT (a), PETG1 (b), PETG2 (c) and PCTT (d) annealed at Tg-20 °C are shown in Fig. 2. The figure presents an endotherm peak at T_g, which corresponds to the enthalpy lost during annealing. Enthalpy loss increases with annealing time in all polyesters along with T_g-onset and peak position, which has been observed previously [23,28,30]. PETG1 and PETG2 show a steady increase in peak height and T_g-onset while the T_g-onset of PETT and PCTT increase non-linearly. Generally, enthalpy loss is first observed after approx. 2 h of annealing, which agrees with the previously reported conclusion that enthalpy stays constant at short annealing times [31]. This indicates that the polyesters undergo some structural rearrangement with constant enthalpy.

The enthalpy loss as function of annealing time at T_g-20, -30 and −40 °C is shown in Fig. 3, illustrating that enthalpy loss increases linearly with the logarithm of annealing time, which is typical behaviour for glassy polymers [30]. A temperature-dependent rate and inhibition time increase, where the enthalpy loss is zero, is also observed.

A small difference is found when comparing the polyesters containing TMCD (PETT and PCTT) to the ones that only contain CHDM (PETG1 and PETG2) as glycol modification . The enthalpy loss in PCTT and particularly in PETT is lower than in PETG1 and PETG2, presenting that TMCD may inhibit enthalpy relaxation. After 24 h at T_g-20 °C the enthalpy loss of PETT and PCTT are 1.2 ± 0.04 and 2.0 ± 0.04 J/g, respectively, where PETG1 and 2 are 2.8 ± 0.02 and 2.8 ± 0.07 J,

respectively. This shows that the rate of enthalpy relaxation is 58 and 27% lower for PETT and PCTT than the PETG1 and PETG2. There are no significant differences between enthalpy relaxation in PETG1 and PETG2 in the tested temperature span, suggesting that the increase in CHDM content from PETG1 to PETG2 does not affect the enthalpy relaxation rate. However, considering the increased enthalpy loss in PCTT compared to PETT, backbone containing CHDM accelerates physical aging compared to that involving EG.

Horizontal shift factors for enthalpy relaxation in PETT obtained by time-temperature superposition are shown in Fig. 4. Similar plots for PETG1, PETG2 and PCTT can be found in Figs. S18–20. The VFT and Arrhenius fitted curves do not illustrate significant differences in ability to capture the trend in shift factors. Even though Arrhenius provides a slightly better fit, the difference is not large enough to confirm from the data presented here.

The VFT parameters and Arrhenius activation energies can be found in Table 4. PETT exhibits the lowest activation energy suggesting that the enthalpy relaxation in this polyester is less accelerated when annealed in the range T_g-40 to T_g-20 °C compared to the CHDM containing polyesters.

3.3. Yield strength

The yield strength data are shown in Fig. 5 as a function of the annealing time at different temperatures. The yield strength increases linearly with the logarithm of annealing time. It can furthermore be seen that higher annealing temperature shifts the curves to shorter annealing times. For PETT, PETG1 and PETG2 an inhibition period is observed, decreasing with increasing annealing temperature. This period is seen most clearly for T_g-40 °C, where it makes up the first 2 h for PETT and the first 24 h for PETG1 and PETG2. For PCTT a yield strength difference is recorded after just 0.5 h of annealing at all the three temperatures. PETT displays the highest yield strength before aging of ~60 MPa and achieves the highest value after aging, ~72 MPa, after 504 h at T_g-30 °C, suggesting strong secondary interactions induced by TMCD compared to CHDM. In PETG1 a similar increase of 11 MPa is found after 504 h at T_g-30 °C, but the yield strength remained below 66 MPa.

Horizontal shift factors for PETT produced by time-temperature superposition with T_g-40 °C as reference temperature is depicted in Fig. 6 with fitted Arrhenius and VFT models. Similar plots for PETG1, PETG2 and PCTT can be found in Figs. S18–20. The VFT parameters and Arrhenius activation energies are shown in Table 4. The decrease in activation energy of 46–90% in polyesters with TMCD compared to polyesters with only CHDM as glycol modification suggests an inhibiting effect of TMCD on physical aging.

3.4. Summary

The temperature dependencies of physical aging manifested by yield strength increase and enthalpy loss have been investigated and fitted with the Arrhenius equation and VFT law. The obtained activation energies and VFT parameters are presented in Table 3. From the studies carried out here, it is unclear if physical aging in the four polyesters exhibit Arrhenius or VFT behaviour, as the two models are almost identical in the tested temperature range.

The Arrhenius activation energies obtained from yield strength increase and enthalpy loss are generally comparable. For PETG1 and PETG2 the difference is only ~3%, which implies a link between the two dynamics. However, for PETT and PCTT, the activation energy for enthalpy relaxation are ~19 and ~107% higher than for yield strength increase, respectively, suggesting a decoupling of the two. The observation of different activation energies obtained from enthalpic and mechanical measurements, especially of PCTT, suggests that the two types of relaxation have different interactions with the structure. For PETT and PCTT the mechanical change is less affected by temperature than the loss of enthalpy, which suggests that the two relaxations are
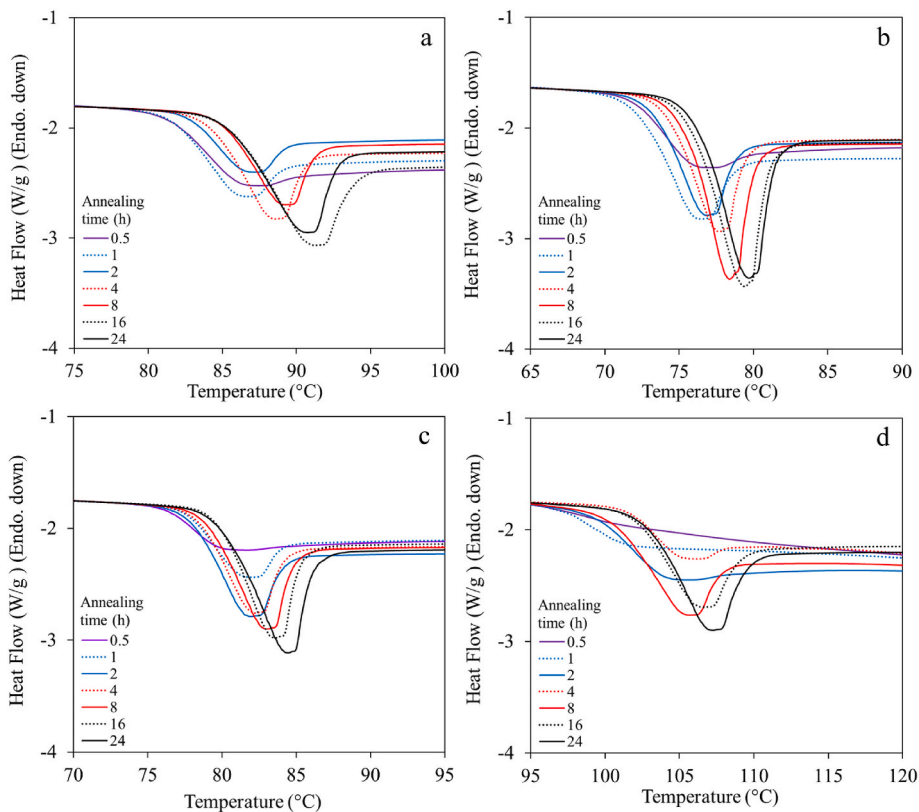
Table 3
Values of T_g, T_f and ΔC_p determined from the first heating scan from DSC.

	T_g [°C]	T_f [°C]	ΔC_p (T_f) [J g^{-1} °C^{-1}]
PETT	94.0 ± 1.4	92.0 ± 1.4	0.173 ± 0.01
PETG1	80.7 ± 2.1	78.8 ± 0.1	0.235 ± 0.02
PETG2	84.5 ± 0.2	82.4 ± 0.7	0.173 ± 0.03
PCTT	108.2 ± 0.3	107.1 ± 0.4	0.210 ± 0.01

Fig. 2. DSC traces representing first heating scan after annealing of samples, PETT (a), PETG1 (b), PETG2 (c) and PCTT (d). Samples were annealed at T_g-20 °C for the times indicated in the figure legend. Curves are shifted vertically to align the plateau below T_g. Partial scans (25 °C around the T_g's) are shown here and full scans in Figure A.10-13.
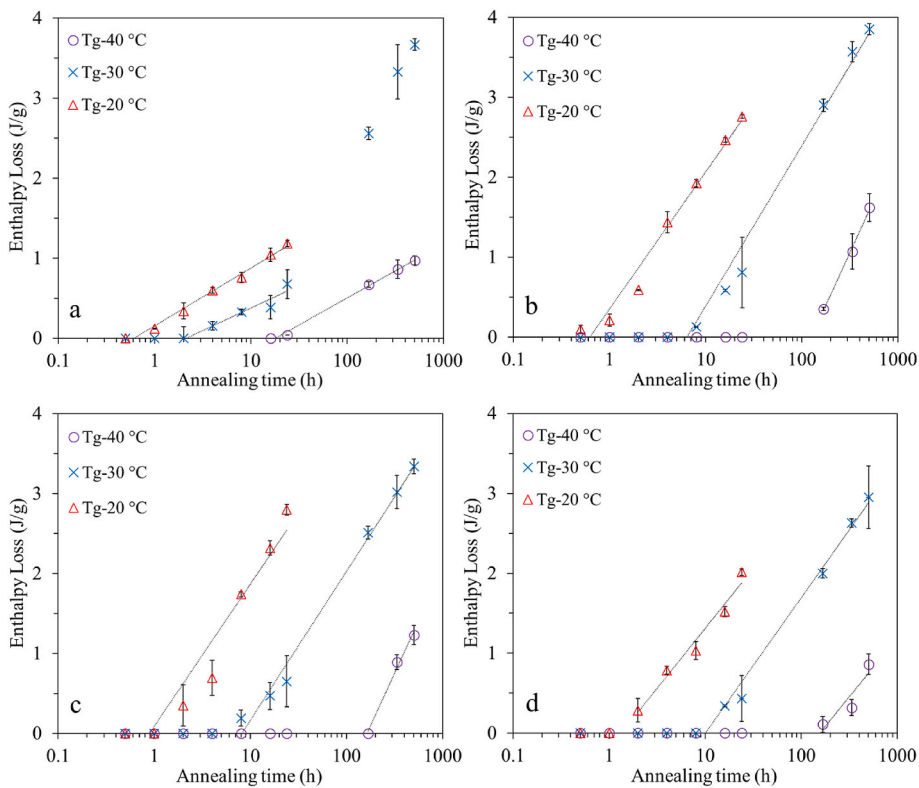

Fig. 3. Enthalpy loss $\Delta H(T_g)$ calculated from DSC traces of PETT (a), PETG1 (b), PETG2 (c) and PCTT (d) after annealing at T_g-20, -30 and −40 °C.
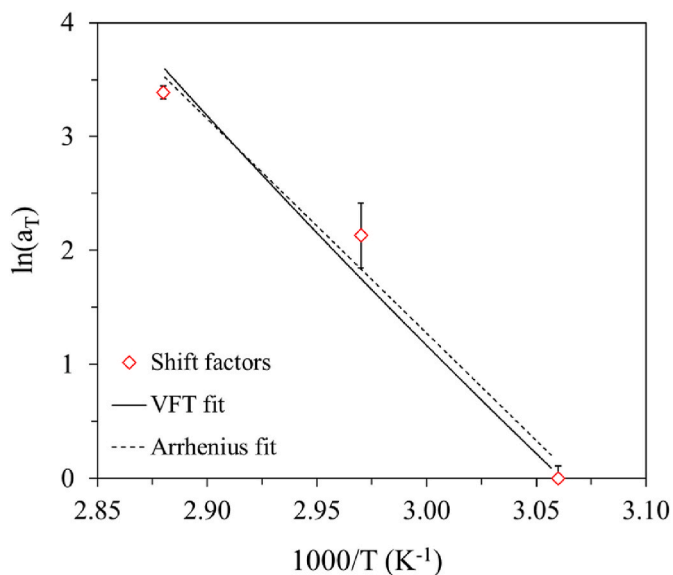
Fig. 4. The logarithm of shift factors versus 1000/T for enthalpy relaxation of PETT.
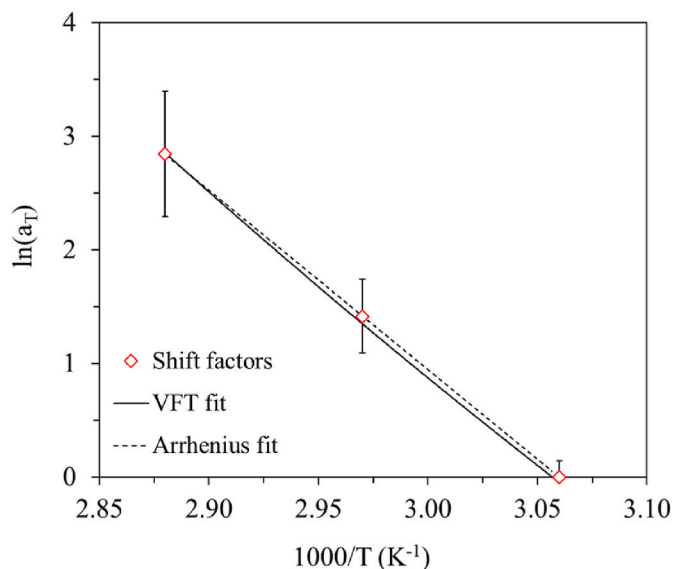

Fig. 6. The logarithm of shift factors versus 1000/T for yield strength increase of PETT.

Table 4

VFT parameters and Arrhenius activation energies, E_a, achieved from fitting yield strength increase and enthalpy loss as function of annealing time and temperature.

|	E_a(Yield strength) [kJ mol^{-1}]	E_a (Enthalpy loss) [kJ mol^{-1}]	B(Yield strength)	B (Enthalpy loss)	D(Yield strength)	D (Enthalpy loss)	T_0(Yield strength)[K]	T_0(Enthalpy loss) [K]
PETT	134 ± 20.8	159 ± 5.0	1.05 10^{-17}	3.56 10^{-21}	0.102	0.120	0.0005	0.0005
PETG1	224 ± 12.5	218 ± 12.5	6.74 10^{-19}	1.17 10^{-19}	0.072	0.795	0.0015	0.0014
PETG2	195 ± 15.8	201 ± 11.6	2.90 10^{-21}	2.48 10^{-21}	0.100	0.101	0.0010	0.0010
PCTT	118 ± 13.3	244 ± 15.0	3.49 10^{-18}	1.54 10^{-20}	0.116	0.077	0.0001	0.0012
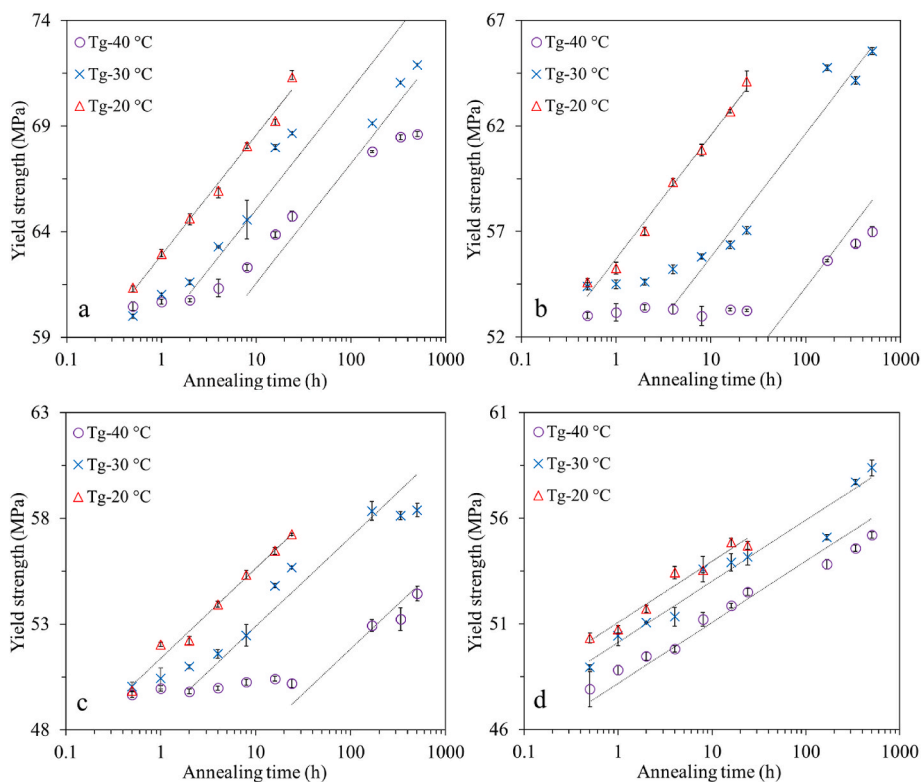
Fig. 5. Tensile yield strength of PETT (a), PETG1 (b), PETG2 (c) and PCTT (d) after annealing at T_g-20, -30 and −40 °C. Lines are created from best logarithmic fit to T_g-20 °C of each polyester and fitted to T_g-30 and -40 °C by changing the intersect.

coupled to the underlying amorphous structure differently. Furthermore, a difference in inhibition period is found between enthalpy and yield strength change, suggesting that structural changes occur before they are measurable in enthalpic experiments. This means, that while the enthalpy stays constant in the early stages of physical aging, the structure rearranges causing mechanical changes. How these rearrangements are permitted and why the enthalpy does not change correspondingly is yet unknown. Since longer annealing times provide a better fit between the two kinetics, expressed as similar Arrhenius activation energies, it is plausible that thermal history of the materials controls the first stage of physical aging.

From this study the correlation between yield strength and enthalpy loss is clearer for the polyesters glycol modified with CHDM instead of TMCD. Furthermore, the thermodynamic equilibrium states of the amorphous phases differs between the investigated copolyesters, suggesting that the mechanical and enthalpic contribution is fundamentally different and that enthalpy loss does not correlate to the yield strength increase.

4. Conclusion

Two related sets of experiments have been carried out independently to investigate the effect of physical aging in four different PET-based copolyesters induced at T_g-20, 30 and 40 °C. We have reported enthalpy relaxation during physical aging, studied by DSC, compared to the effect of physical aging on tensile yield strength. The rates of changes in enthalpy and yield strength depend on both temperature of exposure and backbone rigidity.

The physical aging rate depend on the chemical structure and composition of CHDM and TMCD segment. In the results presented here, structural stiffness and bulkiness decreased physical aging rate measured as both yield strength increase and enthalpy loss. Especially the introduction of TMCD inhibited physical aging.

Generally, the increase in yield strength and enthalpy loss follow Arrhenius and VFT behaviour for all four copolyesters in the tested temperature range. Based on the obtained Arrhenius activation energies, the correlation between yield strength and enthalpy loss is more evident for the polyesters glycol modified with CHDM instead of TMCD suggesting that the relationship between the two phenomena is not independent of chemical structure. Furthermore, this implies that rate and temperature acceleration of physical aging depend on the method of observation.

CRediT authorship contribution statement

Anne Therese Weyhe: Conceptualization, Methodology, Investigation, Formal analysis, Writing – original draft, Writing – review & editing, Funding acquisition. **Emil Andersen:** Conceptualization, Methodology, Writing – original draft, Funding acquisition. **René Mikkelsen:** Supervision, Resources, Funding acquisition. **Donghong Yu:** Supervision, Writing – original draft, Writing – review & editing.

Declaration of competing interest

The authors declare that they have no known competing financial interests or personal relationships that could have appeared to influence the work reported in this paper.

Data availability

Data will be made available on request.

Acknowledgements

Appendix A. Supplementary data

Supplementary data to this article can be found online at https://doi.org/10.1016/j.polymer.2023.125987.

References

[1] R.M. Cywar, N.A. Rorrer, C.B. Hoyt, G.T. Beckham, E.Y.-X. Chen, Bio-based polymers with performance-advantaged properties, Nat. Rev. Mater. 7 (2) (2022) 83–103, https://doi.org/10.1038/s41578-021-00363-3. Feb.

[2] H. Nakajima, P. Dijkstra, K. Loos, The recent developments in biobased polymers toward general and engineering applications: polymers that are upgraded from biobased polymers, analogous to petroleum-derived polymers, and newly developed, Polymers 9 (12) (2017) 523, https://doi.org/10.3390/polym9100523. Oct.

[3] A. Pellis, M. Malinconico, A. Guarneri, L. Gardossi, Renewable polymers and plastics: performance beyond the green, N. Biotech. 60 (Jan. 2021) 146–158, https://doi.org/10.1016/j.nbt.2020.10.003.

[4] M.H. Hassan, et al., The potential of polyethylene terephthalate glycol as biomaterial for bone tissue engineering, Polymers 12 (12) (2020) 3045, https://doi.org/10.3390/polym12123045. Dec.

[5] Z.I. Khan, U. Habib, Z.B. Mohamad, A.M. Raji, Enhanced mechanical properties of a novel compatibilized recycled polyethylene terephthalate/polyamide 11 (rPET/PA11) blends, Express Polym. Lett. 15 (12) (2021) 1206–1215, https://doi.org/10.3144/expresspolymlett.2021.96.

[6] P. Sarda, J.C. Hanan, J.G. Lawrence, M. Allahkarami, Sustainability performance of polyethylene terephthalate, clarifying challenges and opportunities, J. Polym. Sci. 60 (1) (Jan. 2022) 7–31, https://doi.org/10.1002/pol.20210495.

[7] A.K. Singh, R. Bedi, B.S. Kaith, Composite materials based on recycled polyethylene terephthalate and their properties – a comprehensive review, Compos. B Eng. 219 (2021) 108928, https://doi.org/10.1016/j.compositesb.2021.108928. Aug.

[8] W. Loyens, Ultimate mechanical properties of rubber toughened semicrystalline PET at room temperature, Polymer 43 (21) (2002) 5679–5691, https://doi.org/10.1016/S0032-3861(02)00472-X. Oct.

[9] M.K. Eriksen, J.D. Christiansen, A.E. Daugaard, T.F. Astrup, Closing the loop for PET, PE and PP waste from households: influence of material properties and product design for plastic recycling, Waste Manag. 96 (2019) 75–85, https://doi.org/10.1016/j.wasman.2019.07.005. Aug.

[10] A.M. Al-Sabagh, F.Z. Yehia, Gh Eshaq, A.M. Rabie, A.E. ElMetwally, Greener routes for recycling of polyethylene terephthalate, Egypt. J. Pet. 25 (1) (Mar. 2016) 53–64, https://doi.org/10.1016/j.ejpe.2015.03.001.

[11] H. Gao, Y. Bai, H. Liu, J. He, Mechanical and gas barrier properties of structurally enhanced poly(ethylene terephthalate) by introducing 1,6-hexylenediamine unit, Ind. Eng. Chem. Res. 58 (47) (2019) 21872–21880, https://doi.org/10.1021/acs.iecr.9b04953. Nov.

[12] S.K. Burgess, J.E. Leisen, B.E. Kraftschik, C.R. Mubarak, R.M. Kriegel, W.J. Koros, Chain mobility, thermal, and mechanical properties of poly(ethylene furanoate) compared to poly(ethylene terephthalate), Macromolecules 47 (4) (2014) 1383–1391, https://doi.org/10.1021/ma5000199. Feb.

[13] C.J. Kibler, A. Bell, J.G. Smith, Linear Polyesters and Polyester-Amides from 1,4-cyclohexanedimethanol, vol. 25, 1959, 2901466, Aug.

[14] S.R. Turner, Development of amorphous copolyesters based on 1,4-cyclohexanedimethanol, J. Polym. Sci. Part Polym. Chem. 42 (23) (2004) 5847–5852, https://doi.org/10.1002/pola.20460. Dec.

[15] Y. Yu, C. Pang, X. Jiang, Z. Yang, J. Ma, H. Gao, Copolycarbonates based on a bicyclic diol derived from citric acid and flexible 1,4-cyclohexanedimethanol: from synthesis to properties, ACS Macro Lett. 8 (4) (Apr. 2019) 454–459, https://doi.org/10.1021/acsmacrolett.9b00184.

[16] D.R. Kelsey, B.M. Scardino, J.S. Grebowicz, H.H. Chuah, High impact, amorphous terephthalate copolyesters of rigid 2,2,4,4-Tetramethyl-1,3-cyclobutanediol with flexible diols, Macromolecules 33 (16) (2000) 5810–5818, https://doi.org/10.1021/ma000223+. Aug.

[17] K.A. Iyer, Chain mobility, secondary relaxation, and oxygen transport in terephthalate copolyesters with rigid and flexible cyclic diols, Polymer 129 (Oct. 2017) 117–126, https://doi.org/10.1016/j.polymer.2017.09.049.

[18] S. Zhao, J. Zhang, X. Wang, L. Wang, J. Wang, C. Pang, Semiaromatic polyesters from a rigid diphenyl-terephthalic acid: from synthesis to properties, ACS Appl. Polym. Mater. 5 (4) (2023) 2408–2416, https://doi.org/10.1021/acsapm.2c02101. Apr.

[19] E. Andersen, R. Mikkelsen, S. Kristiansen, M. Hinge, Accelerated physical ageing of poly(1,4-cyclohexylenedimethylene-*co*-2,2,4,4-tetramethyl-1,3-cyclobutanediol terephthalate), RSC Adv. 9 (25) (2019) 14209–14219, https://doi.org/10.1039/C9RA00925F.

[20] E. Andersen, R. Mikkelsen, S. Kristiansen, M. Hinge, Real-time ageing of polyesters with varying diols, Mater. Chem. Phys. 261 (2021) 124240, https://doi.org/10.1016/j.matchemphys.2021.124240. Mar.

[21] T. Sang, C.J. Wallis, G. Hill, G.J.P. Britovsek, Polyethylene terephthalate degradation under natural and accelerated weathering conditions, Eur. Polym. J. 136 (2020) 109873, https://doi.org/10.1016/j.eurpolymj.2020.109873. Aug.

[22] L.C.E. Struik, Physical aging in plastics and other glassy materials, Polym. Eng. Sci. 17 (3) (Mar. 1977) 165–173, https://doi.org/10.1002/pen.760170305.

[23] R. Svoboda, J. Málek, Description of enthalpy relaxation dynamics in terms of TNM model, J. Non-Cryst. Solids 378 (Oct. 2013) 186–195, https://doi.org/10.1016/j.jnoncrysol.2013.07.008.

[24] A.V. Cugini, A.J. Lesser, Aspects of physical aging, mechanical rejuvenation, and thermal annealing in a new copolyester, Polym. Eng. Sci. 55 (8) (2015) 1941–1950, https://doi.org/10.1002/pen.24035. Aug.

[25] A.Q. Tool, Viscosity and the extraordinary heat effects in glass, J. Res. Natl. Bur. Stand. 37 (2) (1946) 73, https://doi.org/10.6028/jres.037.033. Aug.

[26] C.T. Moynihan, A.J. Easteal, M.A. Bolt, J. Tucker, Dependence of the fictive temperature of glass on cooling rate, J. Am. Ceram. Soc. 59 (1–2) (Jan. 1976) 12–16, https://doi.org/10.1111/j.1151-2916.1976.tb09376.x.

[27] O.S. Narayanaswamy, A model of structural relaxation in glass, J. Am. Ceram. Soc. 54 (10) (Oct. 1971) 491–498, https://doi.org/10.1111/j.1151-2916.1971.tb12186.x.

[28] N. Doulache, M.W. Khemici, A. Gourari, M. Bendaoud, DSC study of polyethylene terephtalate's physical ageing, in: 2010 10th IEEE International Conference on Solid Dielectrics, IEEE, Potsdam, 2010, pp. 1–4, https://doi.org/10.1109/ICSD.2010.5568072. Juls.

[29] G.D. Liu, J.P. Wu, H.M. Dong, H.Q. Zhang, Nonlinear modification of vogel-fulcher-tamman (VFT) model and its application in enthalpy relaxation of glassy polystyrene, J. Non-Cryst. Solids 528 (2020) 119761, https://doi.org/10.1016/j.jnoncrysol.2019.119761. Jan.

[30] J.M. Hutchinson, S. Smith, B. Horne, G.M. Gourlay, Physical aging of polycarbonate: enthalpy relaxation, creep response, and yielding behavior, Macromolecules 32 (15) (1999) 5046–5061, https://doi.org/10.1021/ma981391t. Jul.

[31] J. Rault, Ageing of glass: role of the vogel fulcher tamman law, J. Phys. Condens. Matter 15 (11) (2003) S1193–S1213, https://doi.org/10.1088/0953-8984/15/11/338. Mar.

[32] K.T. Gillen, R. Bernstein, D.K. Derzon, Evidence of non-Arrhenius behaviour from laboratory aging and 24-year field aging of polychloroprene rubber materials, Polym. Degrad. Stabil. 87 (1) (Jan. 2005) 57–67, https://doi.org/10.1016/j.polymdegradstab.2004.06.010.

[33] K.T. Gillen, M. Celina, R.L. Clough, J. Wise, Extrapolation of accelerated aging data - Arrhenius or erroneous? Trends Polym. Sci. 5 (1997) 250–257.

[34] V. F. Janas and R. L. McCullough, 'The Effects of Physical Aging on the Viscoelastic Behavior of a Thermoset Polyester', p. 20.

[35] E.A. Di Marzio, A.J.M. Yang, Configurational entropy approach to the kinetics of glasses, J. Res. Natl. Inst. Stand. Technol. 102 (2) (1997) 135, https://doi.org/10.6028/jres.102.011. Mar.

[36] P.A. O'Connell, G.B. McKenna, Arrhenius-type temperature dependence of the segmental relaxation below Tg, J. Chem. Phys. 110 (22) (1999) 11054–11060, https://doi.org/10.1063/1.479046. Jun.

[37] J. Zhao, G.B. McKenna, Temperature divergence of the dynamics of a poly(vinyl acetate) glass: dielectric vs. mechanical behaviors, J. Chem. Phys. 136 (15) (2012) 154901, https://doi.org/10.1063/1.3701736. Apr.

[38] S.L. Simon, J.W. Sobieski, D.J. Plazek, Volume and enthalpy recovery of polystyrene, Polymer 42 (6) (2001) 2555–2567, https://doi.org/10.1016/S0032-3861(00)00623-6. Mar.

[39] V.M. Boucher, D. Cangialosi, A. Alegría, J. Colmenero, Time dependence of the segmental relaxation time of poly(vinyl acetate)-silica nanocomposites, Phys. Rev. E 86 (4) (2012), https://doi.org/10.1103/PhysRevE.86.041501, 041501, Oct.

[40] R. Richert, Scaling vs. Vogel–Fulcher-type structural relaxation in deeply supercooled materials, Phys. Stat. Mech. Its Appl. 287 (1–2) (2000) 26–36, https://doi.org/10.1016/S0378-4371(00)00451-9. Nov.

[41] T.G. Fox, P.J. Flory, The glass temperature and related properties of polystyrene. Influence of molecular weight, J. Polym. Sci. 14 (75) (Sep. 1954) 315–319, https://doi.org/10.1002/pol.1954.120147514.

[42] T.G. Fox, P.J. Flory, Second-order transition temperatures and related properties of polystyrene. I. Influence of molecular weight, J. Appl. Phys. 21 (6) (Jun. 1950) 581–591, https://doi.org/10.1063/1.1699711.

[43] T. Hatakeyama, H. Hatakeyama, Effect of chemical structure of amorphous polymers on heat capacity difference at glass transition temperature, Thermochim. Acta 267 (Dec. 1995) 249–257, https://doi.org/10.1016/0040-6031(95)02483-2.

[44] J. Shin, S. Nazarenko, C.E. Hoyle, Effects of chemical modification of Thiol−Ene networks on enthalpy relaxation, Macromolecules 42 (17) (2009) 6549–6557, https://doi.org/10.1021/ma9001403. Sep.

[45] B. Wunderlich, Study of the change in specific heat of monomeric and polymeric glasses during the glass transition, J. Phys. Chem. 64 (8) (1960) 1052–1056, https://doi.org/10.1021/j100837a022. Aug.